2021

Identification of four residues within the TM4 of the 5-HT2A receptor necessary for 5-HT2A·mGlu2 heteromerization

John McGinn

Identification of four residues within the TM4 of the 5-HT_{2A} receptor necessary for 5-HT_{2A}·mGlu2 heteromerization

A Thesis submitted in fulfillment of the requirements for the degree of Master of Science in Physiology and Biophysics at Virginia Commonwealth University

By:

John M. McGinn

B.A. Biology, University of Virginia, 2017

Director: Javier González-Maeso

Professor

Department of Physiology and Biophysics

Virginia Commonwealth University

Richmond, Virginia

December 8, 2021

Acknowledgments

The process of earning a Master's degree and preparing a thesis is time-consuming and arduous – and it is certainly not done singlehandedly. First and foremost, I would like to thank my parents, Michael & Erika McGinn, for their unwavering support and encouragement throughout my studies.

I want to express my deep gratitude to Dr. Javier Gonzalez-Maeso and Dr. Urjita Shah, my research supervisors, for their patient guidance, enthusiastic encouragement, and valuable critiques of this research work. Thank you to my peers for their continued support of my dreams and aspirations and my mentors for pushing and supporting me every step of the way.

I would also like to thank the other members of my Master's committee: Dr. Ian Ramsey and Dr. Montserrat Samso. Their insight, feedback, and advice were influential and essential throughout the process.

Table of Contents

List of Figures iv

List of Abbreviations v

Abstract 6

Chapter 1: Introduction 7
Schizophrenia 7
General GPCR characteristics 9
The 5-HT_{2A}·mGlu2 Heteromeric Receptor Complex 13
Mapping the Heteromeric Interface of $5HT_{2A}$-mGlu2 14
Objective 15

Chapter 2: Research Methods 16
Plasmid Preparation, Amplification, and Sequencing of Constructs 16
Cell culture 16
Transient Transfection of HEK 293 cells 17
Cell Membrane Preparation 17
Co-immunoprecipitation 18
Western Blot 19
Radioligand binding 19
$[Ca^{2+}]_i$ Mobilization Assay 20
Confocal microscopy imagine 21

Chapter 3: Results 22
Sequence alignment 22
5-HT_{2A} TM4 N-terminal Residues Role in Mediating Association with mGlu2 25
Functional Characterization of 5-HT_{2A}-TM4ΔNF 26
Figure 4. Ca2+ mobilization on transiently transfected HEK-293 cells with Fluo-4. 27
Antagonist radioligand saturation 27
Figure 5. [3H] Ketanserin saturation binding. 28
Subcellular Localization of 5-HT_{2A}-ΔTM4NF-mcherry 28
Figure 6 Cytochemistry 5-HT2A-TM4ΔNF in HEK-293 cells. 29

Chapter 4: Discussion 29

Conclusion: 34

References 36

List of Figures

Figure 1: 5-HT_{2A}-TM4ΔNF sequence homology between 5-HT_{2A} and 5-HT2C in TM4

Figure 2: 5-HT_{2A}-TM4ΔNF Immunoblot

Figure 3: Co-immunoprecipitation 5-HT_{2A}-TM4ΔNF + mGlu2

Figure 4: Functional characterization by [^{3}H]ketanserin saturation binding

Figure 5: Ca^{2+} mobilization on transiently transfected HEK-293 cells with Fluo-4

Figure 6: Cytochemistry 5-HT_{2A}-TM4ΔNF + mGlu2

List of Abbreviations

5-HT_{2A}	Serotonin Receptor 2A Subtype
5-HT_{2C}	Serotonin Receptor 2C Subtype
mGlu2	Metabotropic glutamate receptor subtype 2
mGlu3	Metabotropic glutamate receptor subtype 3
WT	Wild-type
Ab	Antibody
BSA	Bovine Serum Albumin
dFBS	Dialyzed Fetal Bovine Serum
DMEM	Dulbecco’s Modified Eagle’s Medium
DPBS	Dulbecco's Phosphate Buffered Saline
GPCR	G protein-Coupled Receptor
LSD	Lysergic Acid Diethylamide
PBST	Phosphate-Buffered Saline + 0.1% Tween 20
SDS-PAGE	Sodium dodecyl Sulfate-Polyacrylamide Gel Electrophoresis
TBST	TRIS-Buffered Saline + 0.1% Tween 20

Abstract

While the etiology is unknown, serotonin and glutamate G protein-coupled receptors (GPCR) neurotransmission dysfunctionality is characteristic of schizophrenia. Previous findings demonstrated that the serotonin 5-hydroxytryptamine 2A (5-HT_{2A}) receptor and the metabotropic glutamate 2 (mGlu2) receptor assemble into a heteromeric complex; however, little is known of the complete structural interface of the heteromer. Through a mutational-based approach, previous research identified Transmembrane domain 4 (TM4) as being responsible for mediating heteromerization in mGlu2 before determining the particular amino acids responsible for the interface. A similar technique was used in this investigation to determine which component of 5-HT_{2A} is responsible for the heterodimeric interface. Here, I identified four residues at the N-terminal of transmembrane domain four essential for the 5-HT_{2A} receptor to form a GPCR heteromer with the mGlu2 receptor in HEK-293 cells. Substitution of these residues (phenylalanine 4.43, leucine 4.44, isoleucine 4.47, and alanine 4.48) leads to a significant reduction of 5-HT_{2A}·mGlu2 receptor complex formation. This finding offers potential targets for future photo-crosslinking investigations to identify the particular residues within the 5-HT_{2A} responsible for mediating the heteromeric interface of the 5-HT_{2A}·mGlu2 complex.

Chapter 1: Introduction

Schizophrenia

Schizophrenia affects 0.3-1.1% of the population and is a persistent, severe, and debilitating mental illness with long-term consequences for patients and their families (Howes and Kapur, 2009). Life expectancy may be reduced by as much as 15 years in schizophrenia patients, with morbidity being considerably more significant than with illnesses such as pulmonary and cardiovascular sickness (Saha *et al*., 2007; Olfson, 2015). A significant contributor to this loss of life is suicide, with studies estimating individuals with schizophrenia have a lifetime suicide risk of 5-10%. (Hor, 2010; Freedman, 2003). However, mortality should not be the sole measure of severity of a disease, as it is not representative of the hardships faced by an individual with a given condition. Disability-adjusted life years (DALY) can be used instead to provide a metric that quantifies the overall burden of illnesses. In conjunction with the World Health Organization and the World Bank, DALY was pioneered by Christopher, Murray, and Lopez, resulting in the first Global Burden of Disease (GBD) study in 1990. According to the most recent GBD study in 2016, schizophrenia accounts for 1.7% of the total DALYs globally and carries the highest disability weight of all disorders in the GBD (Charlson *et al*., 2018; Salomon *et al*., 2015).

Economically, schizophrenia was estimated to cost the United States $155 billion in 2013 through both direct and indirect healthcare costs, totaling $44,773 per individual patient based on a prevalence of 1.0%. When compared to major depressive disorder (MDD), which affects 8.1% of the United States population and indirect costs $210.5 billion ($4,071.8 per MDD patient), the severe economic burden schizophrenia imposes becomes more evident (Greenberg *et al.*, 2015; Wander, 2020)

Schizophrenia, which usually develops during adolescence or early adulthood, can present itself with a wide variety of symptoms, the hallmarks being changes in perception, thought, and behavior. (Owen *et al*., 2016).

The DSM-5 diagnostic criteria for schizophrenia include hallucinations (i.e., sensory perceptions in the absence of concurrent sensory stimuli), delusions (i.e., beliefs firmly maintained despite significant evidence of them being not true), disorganized speech and behavior (e.g., grossly disorganized, frequent derailment or incoherence), and negative symptoms (characterized by loss or deficits of features that are present in healthy individuals) (American Psychiatric Association, 2013). Disability often results from both a combination of negative symptoms and cognitive symptoms (e.g., learning and attention disorders). In addition, relapse may occur because of positive symptoms (characterized by an excess or distortion of normal function), such as suspiciousness, delusions, and hallucinations (Crismon *et al*,. 2014; Patel *et al*,. 2014).

While the etiology of schizophrenia is unknown, it has been demonstrated to involve a variety of structural and neurochemical dysfunctions in multiple brain regions (Ripke *et al.*, 2013), of which abnormalities in neurotransmitter systems have been proposed to contribute significantly (Brish *et al*., 2014).

Overactive dysregulation in the dopaminergic neurotransmitter (DA) system has been the predominant pathophysiological hypothesis of schizophrenia. This stemmed from two observations: 1) first-generation “typical” antidopaminergic antipsychotics primarily as D2 antagonists 2) indirect D2 agonists (amphetamine, phencyclidine, etc.,) induce psychotomimetic effects or exacerbate schizophrenic symptoms by increasing dopamine activity in the subcortical and limbic regions. This overactivity has also been supported by human postmortem findings of

the frontal cortex, which observed increases in D2 receptor expression and D2 mRNA levels, with increased activity in the mesolimbic pathway (Davis *et al*., 1991; Abi-Dargham *et al*., 2000; Tallerico *et al*., 2001).

The roles of other neurotransmitters such as glutamate (Glu) and serotonin (5-HT) in the neuropathology of schizophrenia have started to gain particular attention as being the primary target of second-generation antipsychotics (Miyamoto *et al*., 2005; Conn *et al*., 2009). Furthermore, the psychotomimetic effects of drugs that antagonize the glutamate and serotonin signal recapitulate schizophrenia ethology to a much more accurate extent than drugs that simply stimulate dopamine signaling (Kapur *et al*., 2002; Halberstadt *et al*., 2011).

Many neurotransmitters involved in schizophrenia act through metabotropic G protein-coupled receptors (GPCRs). Serotonin, dopamine, and glutamate are traditionally recognized as molecular targets in this investigation (Patil S *et al*., 2007; Kwan C *et al*., 2021).

General GPCR characteristics

G protein-coupled receptors (GPCRs) are the largest family of cell-surface receptors in the human genome that function to mediate slow synaptic transmission by modulating intracellular signal transduction, through which they regulate an incredible range of physiological processes ranging from cell growth to neurotransmission (Ji et al., 1998; Levoye A et al., 2006; Grundmann et al., 2018).

GPCRs share a common structure comprised of a single polypeptide chain with seven transmembrane (TM) α-helix domains, an extracellular amino-terminal, an intracellular carboxyl-terminal tail, and three cytosolic and extracellular loops. The G proteins associated with

GPCRs are heterotrimeric comprised of an: α-subunit, β-subunit, and γ-subunit. By interacting with other membrane proteins involved in signal transduction, these subunits relay messages within the cell (Rosenbaum *et al*., 2009). While sharing distinct structural characteristics, GPCRs have been classified into five major families according to phylogenetic criteria: Family A (rhodopsin-like), Family B (secretin receptor family), Family C (metabotropic glutamate receptors), Adhesion, and Frizzled/Taste2. Sequence homology within these families is at least 40%, with the greatest homology at the transmembrane domain. (Vassilatis *et al*., 2003; Bjarnadóttir *et al*., 2006)

GPCRs can further be categorized by downstream signaling pathways depending on the α subunit: $G_{i/o}$, $G_{s/olf}$, $G_{q/11}$, and $G_{12/13}$. As the name suggests, in response to ligand binding, GPCRs activate heterotrimeric guanine nucleotide-binding proteins (G proteins), stimulation of which results in a dissociation of the Gα subunit from the Gβγ dimer and allows the subunits to activate or inhibit various effectors. $G_{s/olf}$ (stimulatory) and $G_{i/o}$ (inhibitory) pathways regulate cAMP-dependent signaling by either stimulating or inhibiting adenyl cyclase activity. The $G_{q/11}$ coupled pathway operates via phospholipase C-β enzymes, which hydrolyzes phosphatidylinositol 4,5-bisphosphate (PIP_2) to diacylglycerol (DAG) and inositol 1,4,5- trisphosphate (IP_3). Hydrophilic IP_3 diffuses into the cell and acts as a second messenger to release stored calcium from the endoplasmic reticulum lumen into the cytoplasm. Whereas DAG acts as a second messenger that activates protein kinase C (PKC). $G_{12/13}$ stimulates small GTPase downstream signaling (Moghaddam *et al*., 2004; Liu *et al*., 2021).

Comprehensive research on GPCRs led to the identification of an orthosteric site for endogenous ligand binding as well as several allosteric sites that can modulate response: Positive Allosteric Modifiers (PAMS) and Negative Allosteric Modifiers (NAMS) (Foster *et al*., 2017). Due to their

central roles in many cellular functions and numerous binding sites, GPCRs are an important therapeutic target, with different reports suggesting that between 30 and 40% of FDA-approved drugs target GPCRs (Wise *et al*., 2002; Brink *et al*., 2004).

Initially, GPCRs were thought to exist and function as monomeric structural units that couple to G-proteins in a 1:1 stoichiometric ratio. (Liang Y *et al*., 2017) This model is supported by evidence that purified monomeric β2-adrenoreceptor (Family A) reconstitutes in a phospholipid bilayer is sufficient for fully functional G protein activation (Whorton *et al*., 2007; Kuszak *et al*., 2009).

However, over the last decade, the notion that these receptors function exclusively as monomeric proteins has been challenged, with indications that GPCRs can exist and function as dimers or even higher-order oligomers. Investigation into Family A, D2 receptors indicated the receptor requires two structural units to one G-protein to be maximally activated by a single bound ligand (Han *et al.*, 2009). Additional evidence suggests class C metabotropic Glutamate (mGlu) and GABA receptors-act as obligate homodimers, suggesting dimerization is crucial for receptor function (Kniazeff *et al*., 2011).

GPCRs may also undergo heterodimerization. Initial evidence for this model came from studies of the α2-adrenoreceptor and M3 muscarinic receptor in which two mutant chimeras were generated with TM-6 and TM-7 exchanged between α_{2C} and M_3. This revealed that only when co-transfecting the α_2/M_3 and M_3/α_2 chimeras resulted in stimulation, suggesting the two receptors are intricately connected, and the presence of all transmembrane domains was necessary and sufficient for signaling, regardless of which specific receptor they were inserted in (Zeng *et al*., 2000).

Perhaps the most eloquent example of heterodimerization is the interaction between GABAB-R1 and GABAB-R2 subunits in forming a fully functional $GABA_B$ (γ-aminobutyric acid type B) receptor. Functional membrane receptors were created by co-expression of recombinant GABAB-R1 and GABAB-R2 plasmids but not by expressing each recombinant plasmid alone. Further studies exploring this model revealed $GABA_B$-R1 appears to determine the pharmacological properties of the receptor, while $GABA_B$-R2 is essential for the proper expression of $GABA_B$-R1 on the plasma membrane. (Filippov *et al*., 2000; Jones *et al*., 2000)

Heterodimerization involving two fully functional GPCRs from distinct families has also been well established. κ and δ opiate receptors have been shown to form a fully functional heterocomplex receptor that exhibits distinct functional and ligand-binding characteristics distinct from those of either receptor alone (Jordan & Devi, 1999). 5-HT_{2A} and D2 have also been shown to form a functional heterocomplex with ligands conveying different effects on downstream signaling depending on whether homo- or hetero-dimers are present. (Łukasiewicz *et al*., 2010) Additionally, Family A 5-HT_{2A} and Family C mGlu2 receptors have been shown to form a functional heterocomplex in the mammalian brain and tissue culture preparations. (González-Maeso *et al*., 2008; Rives *et al*., 2009; Moreno *et al*., 2012).

There are several ways that a heterocomplex interaction can be assessed. Co-immunoprecipitation (Co-IP) assays are robust measures to determine whether two proteins interact. Co-IP is performed by binding one of the proteins of interest with a magnetic bead, then washing away all proteins that are not bound to the antibody-bead-protein complex, followed by immunoblot probing for the second protein of interest. If the two proteins are part of the same protein complex, then there would be an immunoreactive signal detected for the protein that was not directly bound to the magnetic bead (Tang *et al*., 2018). However, there are also alternative

methods to address GPCR complex formation, including Förster (Fluorescence) Resonance Energy Transfer (FRET) and Bioluminescence Resonance Energy Transfer (BRET). FRET is a technique where after excitation with a laser, an excited donor molecule (e.g., cyan fluorescence protein) transfers resonance energy to an acceptor molecule (e.g., yellow fluorescence protein), producing a highly distance-dependent fluorescence. Therefore, this can accurately measure the molecular proximity of two proteins at angstrom distances (10-100 Å) (Sekar et al., 2003). BRET is a very similar technique to FRET; however, the resonance energy transfer is not between two fluorescent proteins but rather between a bioluminescent donor and a fluorescent acceptor and therefore does not require an excitation source (Dimri *et al*., 2016).

The 5-HT_{2A}·mGlu2 Heteromeric Receptor Complex

Abnormalities in the serotonin and glutaminergic system have been observed in schizophrenia patients compared to neuropsychiatric healthy control subjects. Postmortem and neuroimaging studies suggest an increase in $G_{q/11}$-coupled 5-HT_{2A} receptor density with concurrent decreases in $G_{i/o}$-coupled mGlu2/3 receptor density and treatment with second-generation antipsychotic drugs decreases density to control levels (Gonzalez-Maeso et al., 2008). This has similarly been verified in a rodent model where chronic treatment with second-generation antipsychotics, clozapine and risperidone, downregulated 5-HT_{2A} cortical neurons. (Gonzalez-Maeso et al., 2008; Kurita *et al*., 2012). Additionally, rodent studies revealed that the administration of classic serotonergic psychedelics in mGlu2 -/- knock-out mice eliminated the hallucinogenic-specific signaling component, suggesting this pattern of 5-HT_{2A}, mGlu2 density may predispose psychosis (Gonzalez-Maeso, 2008).

Previous findings have also demonstrated cross-talk between the $G_{q/11}$-coupled 5-HT_{2A} and the $G_{i/o}$-coupled mGlu2 receptors, showing they form a heteromeric complex via which the 5-HT_{2A}·mGlu2 complex incorporates both serotonin and glutamate signaling to modulate downstream signaling and behavioral changes (Moreno, 2016). Further studies have indicated that in response to endogenous ligands (glutamate and serotonin), the 5-HT_{2A}·mGlu2 heteromeric complex functions to establish a $G_{i/o}$-$G_{q/11}$ balance, which is believed to underlie the therapeutic action of mGlu2 activators and 5-HT_{2A} antagonists. Classic psychedelics such as LSD, Mescaline, and Psylocibin, have been shown to shift the signaling balance towards a more psychosis-like condition, while on the other hand, second-generation antipsychotics have been shown to recover the $G_{i/o}$/$G_{q/11}$ imbalance (Fribourg *et al*., 2011).

This heteromeric complex allows for a plethora of therapeutic targets to allow for more deliberate modulation intracellular signal, rather than each individual GPCRs (Wootten *et al*., 2018).

Mapping the Heteromeric Interface of 5HT_{2A}-mGlu2

Within the 5-HT_{2A}·mGlu2 complex, the structural mechanisms responsible for forming the oligomer are poorly understood, as is/are the molecular mechanism(s) responsible for cross-talk. In the investigation into the mechanism by which 5-HT_{2A}·mGlu2 heterocomplex modulates downstream signaling, the structure of the heteromeric interface must be considered. Several studies have used a mutational-based approach to examine whether a direct mechanism contributes to cortical cross-talk between the two receptor systems (Moreno *et al*., 2012)

Co-immunoprecipitation assays of human brain cortex samples and transfected HEK-293 cells with antibody epitope tags verified 5-HT_{2A} and mGlu2, but not mGlu3, form part of the same

protein complex (Gonzalez-Maeso et al., 2008). Due to the sequence homology between mGlu2/3, mutant chimeras with non-homologous amino acid residues of mGlu3 were inserted into mGlu2 in order to disrupt the heteromeric assembly. Through this method, researchers identified three residues at the intracellular end of TM4 (Alaine 4.40, Alanine 4.44, and Alanine 4.48), which are necessary to form the 5-HT_{2A}·mGlu2 receptor heterocomplex. Additionally, when the TM4 residues of mGlu2 were inserted into the mGlu3, it was sufficient for signaling cross-talk to occur (Moreno *et al*., 2012).

As there is similar discrimination found between the 5-HT_{2A} and 5-HT_{2C} (which does not form a protein complex with mGlu2), additional investigations utilizing a similar mutational chimeric method to the one described above indicated the TM4 domain of 5-HT_{2A} is necessary for the heterocomplex to form. (Moreno *et al*., 2016.)

Objective

With abundant research highlighting the biological relevance of the 5-HT_{2A}·mGlu2 heterocomplex in modulating signaling, the complete structural interface between the two GPCRs remains unknown.

While the residues in mGlu2 responsible for dimerization have been identified, the residues in 5-HT_{2A} remain unidentified, having only been limited down to the TM4 domain. I hypothesize that the residues in the N-terminal half of 5-HT_{2A} are responsible for mediating the formation of a heterocomplex with mGlu2.

This was assessed using a heterologous expression system in human embryonic kidney cells (HEK-293). A 5-HT_{2A} chimera mutated to include four aligned residues from $5HT_{2C}$ along the

TM4 of 5-HT_{2A} closest to the N terminus (5-HT_{2A}-TM4ΔNF) was co-expressed with mGlu2 to attempt to disrupt the binding interface of the heteromer.

The four 5-HT_{2A} residues mutated (phenylalanine 4.43, leucine 4.44, isoleucine 4.47, and alanine 4.48) were chosen to start this investigation because these residues i) are different between 5-HT_{2A} and 5-HT_{2C}, and ii) are located facing towards the lipid bilayer according to the recent crystal structure of the 5-HT_{2A} (Kimura *et al*., 2019)

Disruption of the heterocomplex was evaluated using a co-immunoprecipitation followed by immunoblotting. Further characterization of the mutant chimera was also performed to confirm level of expression, cellular localization and function homology to WT 5-HT_{2A}.

Chapter 2: Research Methods

Plasmid Preparation, Amplification, and Sequencing of Constructs

The constructs pcDNA3.1-c-Myc-5-HT_{2A}-mCherry and pcDNA3.1-HA-mGluR2-mCitrine, described previously (Moreno *et al*., 2016), and 5-HT_{2A}-TM4ΔNF were obtained (Kareem, 2020). The primer used for sequencing of Mutant construct (5-HT_{2A}-TM4ΔNF) was: 5'-AGC TGA TAT GCT GCT GGG TT -3'. Following sequence verification, constructs were transformed into XL1-Blue Supercompetent Cells (Agilent Technologies; CN: 200236) before purification and amplification by Plasmid Maxi Prep (QIAGEN).

Cell culture

Human Embryonic Kidney (HEK)-293 cells were used for transfection and cultured in a 5% CO_2 at 37°C in Medium A, DMEM (Dulbecco's Modified Eagle's Medium; 4.5 g/L glucose, L-

glutamine, sodium pyruvate) supplemented with 10% (v/v) dialyzed fetal bovine serum (dFBS) (Thermo Fischer Scientific; CN: 26400044) and 1% (v/v) Penicillin-Streptomycin (Thermo Fischer Scientific; CN: 15140122) (except immediately prior to transfection, as noted below). Cells underwent passages every 2-3 days, using fresh Medium A in a ratio between 1:8 and 1:12, to keep the cells in their exponential growth phase and never passaged higher than 20 times.

Transient Transfection of HEK 293 cells

48hr before transfection, HEK-293 cells were split and cultured in DMEM supplemented with 10% (v/v) dFBS only. All Transient transfections were conducted with Lipofectamine 3000 (Invitrogen; CN: L3000001) using a Lipofectamine 3000 to plasmid ratio of 1:1.5 and performed according to the manufacturer's recommendations. A total of 6 μg/plate of plasmid DNA was used in each single transfection. This includes the individual transfection of the constructs, c-Myc-5-HT_{2A}-mCherry, and c-Myc-5-HT_{2A}-TM4ΔNF-mCherry. A total of 12 μg of DNA was used in each co-transfection with a plasmid ratio of (1:2), 4 μg of which were vector, 5-HT_{2A} receptor, or mutant 5-HT_{2A} receptor DNA and 8 μg of which was DNA construct HA-mGluR2-mCitrine. This includes co-transfection of constructs c-Myc-5-HT_{2A}-TM4ΔNF-mCherry with HA-mGluR2-mCitrine, and c-Myc-5-HT_{2A}-mCherry with HA-mGluR2-mCitrine. 24hr after transfection, media was removed and replaced with DMEM supplemented with 10% (v/v) dFBS and 1% (v/v) Penicillin-Streptomycin, for an additional 24hr before harvesting.

Cell Membrane Preparation

48 Hours following transfection, cells were harvested with Dulbecco's Phosphate-Buffered Saline, 1X without calcium and magnesium (DPBS) (Corning; CN: 21031CV). The resulting cell pellets were frozen at –80°C before being prepared into membranes. A Teflon homogenizer was

used to homogenize the cell pellet (50 ups/downs) in 10ml Tris-HCl 1x (50 mM Tris-HCl, pH 7.4). Homogenized tissue was spun for 5 min at 1,000 × *g* (4°C) and the pellet was discarded. The supernatant was spun for 15 min at 40,000 × *g*. Subsequent pellet was washed with 500 µl Tris-HCl and spun again for 15 min at 40,000 × *g*. The pellet was resuspended in 500µl of Tris-HCl and transferred to a 1.7 ml Eppendorf tube, then spun at 18,000 × *g* in a microcentrifuge for 15 min at 4°C. The Tris-HCl 1x was removed, and the pellet was either used or stored at −80°C until use.

Co-immunoprecipitation

Co-immunoprecipitation was conducted using 600µg of prepared cell membrane. Protein Assay (Bio-Rad; CN: #5000006) was performed to normalize the amount of protein. Membranes were resuspended with 500µl RIPA buffer (50 mM HEPES, 150 mM NaCl, 5mM EDTA, and Mini EDTA-free Protease Inhibitor Cocktail tablet (Roche Applied Sciences; CN: 04693159001), pH 7.4) and allowed to solubilize with 500µl Solubilization buffer (RIPA buffer supplemented with 1% SDS and 2% Triton X-100 (Fischer Scientific; CN: BP151-500)) by incubation on a rotating mixer at 4 °C for 1hr. Cells were incubated on a rotating mixer with Protein A/G PLUS-Agarose immunoprecipitation beads (Santa Cruz Biotechnology; CN: sc-2003) at 4 °C for 30 minutes to account for non-specific binding. 100µl of the cell lysates was saved for Total Protein control, and the remainder was then incubated with immunoprecipitation beads conjugated to c-HA-Tag-Mouse Ab (diluted 1:1000; Cell Signaling Technology; CN: 3724) at 4 °C for 18 hours. The beads were washed at 4 °C three times in RIPA buffer. Immunoprecipitated proteins were then eluted from the beads by resuspension in 20 µl Solubilization buffer, followed by western blotting.

Western Blot

Samples were mixed with 5µl 5x Laemmli buffer and heated for 5 min at 97 °C. Proteins were resolved by 12% SDS-PAGE and transferred to nitrocellulose membranes by electroblotting. Nitrocellulose blots were washed with TBST (150 mM NaCl, 50 mM Tris-Cl, and 0.1% Tween 20, pH 7.6) before incubating the membrane in Blocking Buffer (TBST, 2.5% nonfat dry milk, 0.5% BSA) for 1hr at room temperature. Nitrocellulose blots were then incubated (overnight at 4° C) with c-myc-Tag-Mouse Ab (diluted 1:1000; Cell Signaling Technology; CN: 9B11). Following six washes with TBST, blots were incubated with Anti-Mouse IgG Horseradish peroxidase (HRP) conjugated secondary Ab (1:5000; ACCURATE Chemical Science Corp.) After incubation, blots were washed six more times with TBST for 30 minutes and developed using enhanced chemiluminescence detection (SuperSignal™ West Pico PLUS Chemiluminescent Substrate; Thermo Fischer Scientific) in accordance with manufacture instructions. Immunoreactive bands were analyzed using ChemiDoc Imaging System and Image Lab (Bio-Rad Laboratories). Final data of Co-immunoprecipitation are expressed as a ratio of the relative density of the 250kDa band to its respective 250 kDa total protein band. Final data for characterization of immunoblot signal is expressed as the 250 kDa was normalized to β-actin. Observed differences were considered statistically significant if P-values were below 0.05.

Radioligand binding

Saturation binding assays were performed with the 32µg prepared cell membranes and [^{3}H]ketanserin (22.8 Ci/mmol; PerkinElmer; CN: NET1233), then incubated in Tris-HCl for 1hr at 42°C. The following [^{3}H]ketanserin concentrations were used: 10 nM, 5 nM, 2.5 nM, 1.0 nM, 0.5 nM, 0.25 nM, 0.125 nM, 0.0625 nM, all in duplicate for total and non-specific (three reactions

at each concentration were measured). Non-specific binding was determined by incubating the reactions with 100μM methysergide (Tocris; CN: 1064); two samples were pooled for each assay. Protein Assay (Bio-Rad; CN: #5000006) was performed to normalize the amount of protein in each assay. Reactions were harvested by vacuum filtration through Glass fiber Filtermat A (PerkinElmer) (3× 50 mM Tris-HCl, pH 7.4) and counted by liquid scintillation using a PerkinElmer 2450 MicroBeta^2. Data analyses were performed using Microsoft Excel and GraphPad Prism v8.0 (GraphPad software, San Diego, CA, USA). K_D and B_{max} were determined by a saturation binding analysis, $Y = \frac{B_{max} \times K_D}{K_D + X}$

$[Ca^{2+}]_i$ Mobilization Assay

Functional signaling was assessed by measuring Ca^{2+} release in the presence of serotonin (100μM, 10μM, 1μM, 100nM, 10nM, 1nM, 0.1nM, 0nM) in 5-HT_{2A}-TM4ΔNF or WT 5-HT_{2A} cells. The day before the assay, 50,000 (5-HT_{2A}) or 50,000 (5-HT_{2A}-TM4ΔNF) cells/50 μL were seeded in poly-D-lysine coated (1mg/ml) 96-well black plates (Greiner 781091). The cells were incubated with 50μl 3 μM Fluo 4 Direct (Thermo Fisher Scientific; CN: F10471) in imaging solution (5 mM KCl, 0.4 mM KH_2PO_4, 138 mM NaCl, 0.3 mM Na_2HPO_4, 2 mM $CaCl_2$, 1 mM $MgCl_2$, 6 mM glucose, 20 mM HEPES, pH 7.4) supplemented with pluronic acid (10% solution in DMSO) for 1 h at 37˚C, as described in the manufacturer's instructions. Changes in fluorescence due to intracellular Ca^{2+} mobilization were measured using a FlexStation® plate reader (Molecular Devices) with λex 494 nm and λem 525 nm. Baselines were recorded every 2 s for 30 s. Serotonin was added at 30 s; reading started at 90 s after serotonin transfer, reading every 1 s for a total of 180 s. The fluorescence was a measure of intracellular calcium and was normalized to basal fluorescence using SoftMax Pro (Molecular Devices, Wokingham, UK).

Functional data was analyzed by nonlinear regression to generate concentration-response curves and EC_{50} values by Prism V8.0 software, (Y=Bottom + (Top-Bottom) / (1 + 10 ^ (($LogEC_{50}$-X)*HillSlope)(GraphPad Software, San Diego, CA, USA).

Confocal microscopy imagine

Confocal microscopy imaging was performed on pcDNA3.1-c-Myc-5-HT_{2A}-mCherry and pcDNA3.1-c-Myc-5-HT_{2A}-TM4ΔNF-mCherry transfected HEK 293 cells. Samples were fixed in pre-cooled 4% paraformaldehyde in 1x PBS for 30 minutes, then washed twice with 1X PBS before incubating the membrane in Blocking Buffer (1x PBS, 5% BSA) for 2hr. Cells were then stained with 1:10,000 dilution Hoechst 3342 (20mM) (Thermo Fischer Scientific; CN: 62249) for 15 minutes, then washed two times in Phosphate-Buffered Saline (137 mM NaCl, 2.7 mM KCl, 8 mM Na_2HPO_4, and 2 mM KH_2PO_4) (10 minutes for each wash). Coverslips were transferred to a microscope slide and mounted (Invitrogen ProLong™ Diamond Antifade Mountant) for microscopic fluorescence visualization. Images were acquired using a Zeiss LSM710 laser-scanning confocal microscope (Carl Zeiss AG, Jena, Germany) with Airyscan (Plan-Apochromat, objective 63×, Numerical Aperture 1.4). The zoom images are digitally cropped using the same objective at 2x zoom. Microscopy was performed at the VCU Microscopy Facility, supported, in part, by funding from NIH-NCI Cancer Center Support Grant P30 CA016059.

Chapter 3: Results

Sequence alignment

Sequence analysis was performed to corroborate whether the 5-HT_{2A}-TM4ΔNF chimera was mutated to contain 5-HT_{2C} TM4 N-terminal residues. All residues were identified using the Ballesteros-Weinstein sequence-based numbering system. This revealed successful replacement of WT 5-HT_{2A} residues phenylalanine 4.43, leucine 4.44, isoleucine 4.47, and alanine 4.48 with the isoleucine 4.44, methionine 4.55, alanine 4.47, and isoleucine 4.48 found in WT 5-HT_{2C} (Fig 1).

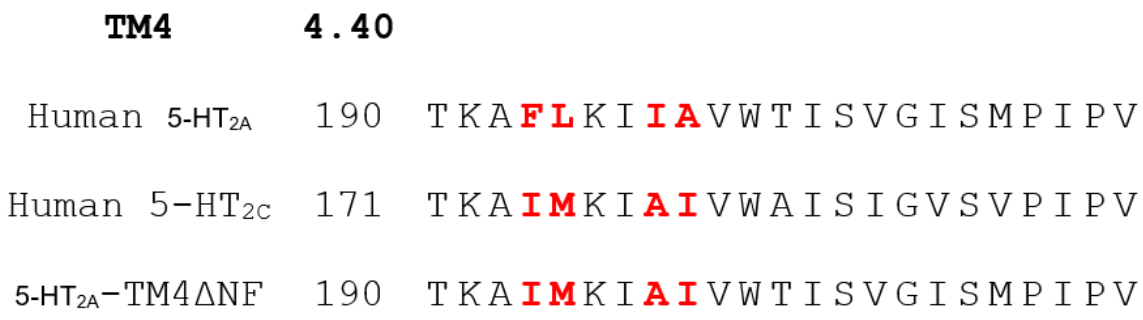

Figure 1. 5-HT_{2A}-TM4ΔNF sequence homology between 5-HT_{2A} and 5-HT_{2C} in TM4. *Amino acid sequence alignment of the transmembrane domain 4 (TM4) of Human 5-HT_{2A}, 5-HT_{2C}, and 5-HT_{2A}-TM4ΔNF receptors. All residues were identified by the sequence-based numbering system by Ballesteros-Weinstein. Residues that are different between 5-HT_{2A} and 5-HT_{2C} in N-terminal TM4 are highlighted in red, with the 5-HT_{2A}-TM4ΔNF mutant sequence alignment at the bottom.*

Characterization by Immunoblot

To assess whether the c-myc-5-HT_{2A}-TM4ΔNF receptor was expressing itself properly, and there was no misfolding, immunoblot assays were performed to test whether the molecular weight of c-myc-5-HT_{2A}-TM4ΔNF is equivalent to 5-HT_{2A}. Immunoblot assays were performed

in membrane lysates of HEK-293 cells transiently transfected with these two constructs. Anti-c-myc immunoreactivity was detected as a mixture of a 53kDa band and a band of approximately 250 kDa corresponding to the size anticipated for a 5-HT_{2A} monomer and oligomer, respectively (Fig. 2). There was no significant difference seen in c-myc immunoreactivity between the c-myc-$5HT_{2A}$-TM4ΔNF and c-myc-5-HT_{2A} 250 kDa oligomer when analyzed by Student's unpaired t-

test (t = 0.6098, df = 4, $P > 0.05$). This suggests an equivalent molecular weight of the 5-HT_{2A}/5-HT_{2C} construct.

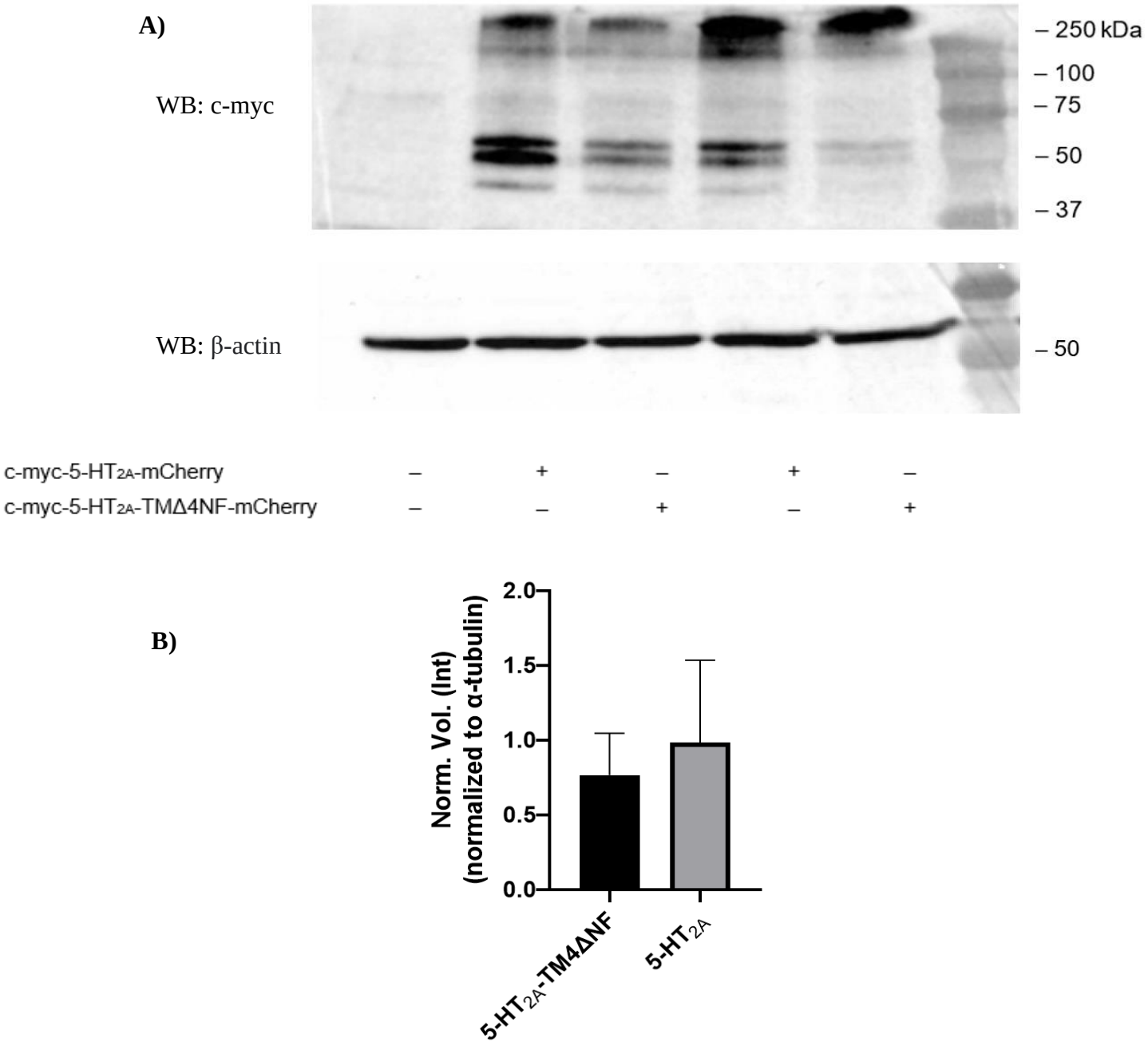

Figure 2 Immunoblot assay. *A) Representative Western blot for 5-HT2A and 5-HT2A-TM4ΔNF. B) Histogram of immunoreactivity (after normalization) of 250 kDa 5-HT2A and/or 5-HT2A-TM4ΔNF. Normalized to β-actin. Error bars indicate S.E.M., significance determined by unpaired Student's t-test. (n = 3; independent experiments performed in duplicate)*

5-HT_{2A} TM4 N-terminal Residues Role in Mediating Association with mGlu2

Co-immunoprecipitation was performed using anti-HA antibodies in plasma membrane preparations of HEK-293 cells transfected to express the HA-mGlu2 together with the c-myc-5HT_{2A}-TM4ΔNF receptors. Immunoblot analysis of co-immunoprecipitated material revealed anti-c-myc immunoreactivity was detected at ~ 250 kDa band, this corresponding to the size of the 5-HT_{2A} oligomer.

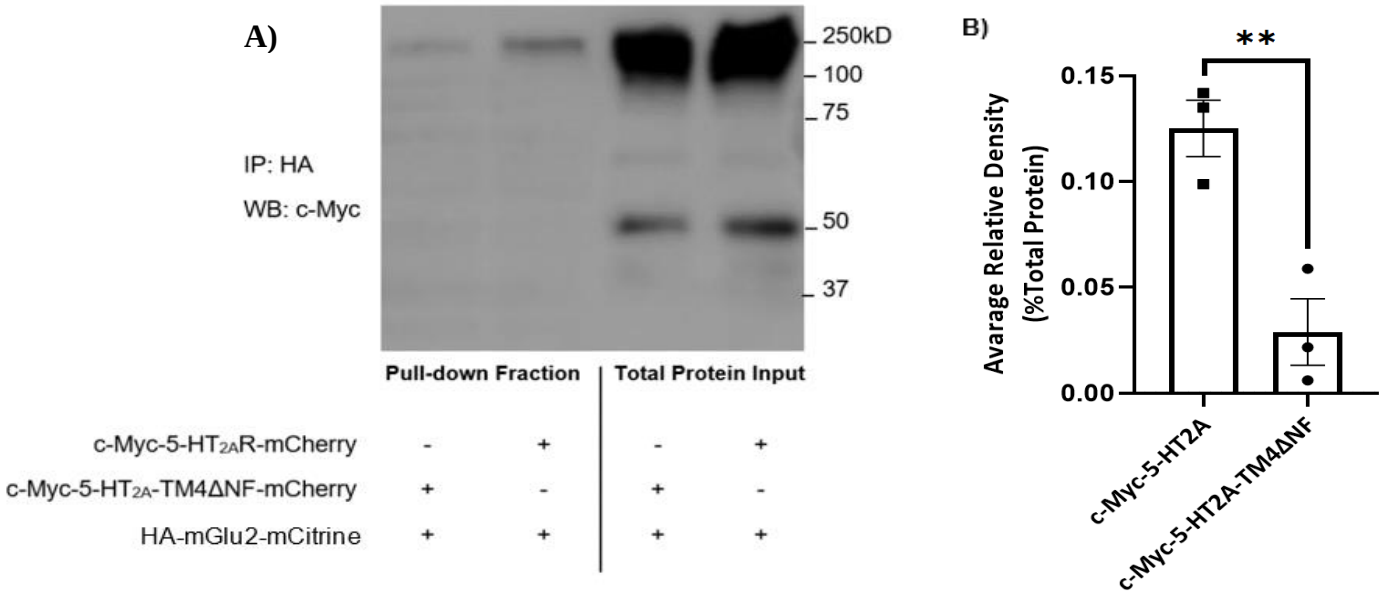

Figure 3. Co-immunoprecipitation 5-HT_{2A}-TM4ΔNF + mGlu2. *A) Western blots showing results of immunoprecipitation with HA-tagged Ab, Wb c-Myc Ab. B) Histogram shows average relative densitometric, from three replicates, normalized to the total protein control before immunoprecipitation. Error bars indicate S.E.M. significance determined by unpaired Student's t-test. The figure shows representative images of three independent experiments.*

Interestingly, substitution of residues F4.43, L4.44, I4.47, and A4.48, in 5-HT_{2A} with the I4.44, M4.55, A4.47, and I4.48 in 5-HT_{2C} (5-HT_{2A}-ΔTM4NF) significantly reduced co-immunoprecipitation with mGlu2 (n=3 unpaired Student's t test (t = 4.687, df = 4, *P* = .009) (Fig. 3).

Functional Characterization of 5-HT_{2A}-TM4ΔNF

In light of the ΔTM4NF mutation's apparent role in mediating the heteromeric interface, further characterization assays were performed to assess functional homology with 5-HT_{2A}. As noted above, 5-HT_{2A} is a $G_{q/11}$ coupled GPCR which, when stimulated, produces a transient increase in the concentration of intracellular Ca^{2+}. An intracellular calcium mobilization assay performed in c-myc-5HT_{2A}-TM4ΔNF transfected HEK-293 cells revealed 5-HT produced a concentration-dependent increase of signal, corresponding to that observed in 5-HT_{2A} (Fig. 4) (EC_{50}: 5-HT_{2A} -ΔTM4NF: 5.6 nM; 5-HT_{2A}: 6.9 nM. E_{max} = 5-HT_{2A} -ΔTM4NF: 98.89; 5-HT_{2A}: 100.2) Analyzed by nonlinear regression to generate concentration-response curves and analysis by unpaired Student's t-test showed no significance (P = .997). As there was no Ca^{2+} mobilization detected in untransfected HEK-293 cells, it can be assumed that the transient increase observed in Fig. 4 is due to the presence of either 5-HT_{2A} -ΔTM4NF or 5-HT_{2A} constructs.

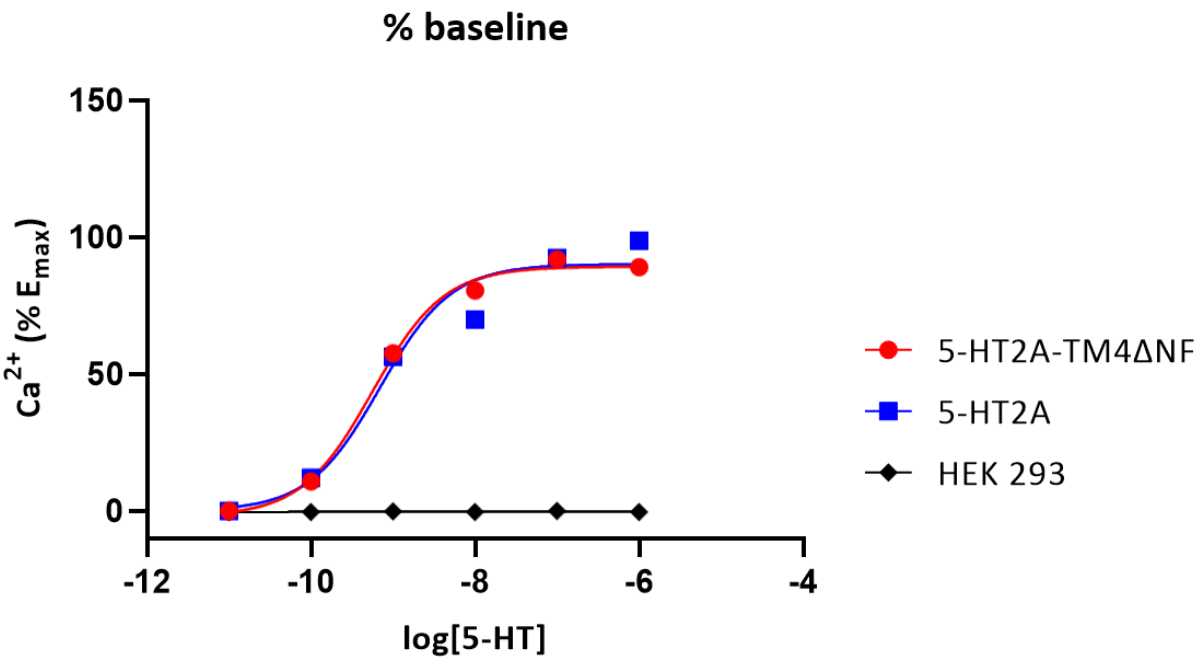

Figure 4. Ca2+ mobilization on transiently transfected HEK-293 cells with Fluo-4. *Concentration dependent Ca^{2+} mobilization for serotonin in transiently transfected HEK-293 cells expressing 5-HT_{2A}-ΔTM4NF or 5-HT_{2A} (50,000 cells/well). All concentration responses represent the mean of two independent experiments, each performed in triplicate wells (n = 2). The SEM values are not presented because n = 2.*

Antagonist radioligand saturation

5-HT_{2A} -ΔTM4NF and 5-HT_{2A} membrane preparations were subjected to saturation analysis with the high-affinity antagonist [^{3}H]ketanserin to determine receptor density. Nonlinear analysis of binding fitted to a saturation curve showed no significant difference in K_D (binding affinity) or Bmax (receptor density) (Bmax: 5-HT_{2A} -ΔTM4NF: 223.0 ± 23.32 fmol/mg; 5-HT_{2A}: 211.3 ± 27.01 fmol/mg. K_D: 5-HT_{2A} -ΔTM4NF: 6.129 ± 1.260 nM; 5-HT_{2A}: 6.784 ± 1.648 nM) (n=3 per group). These results further suggest 5-HT_{2A} -ΔTM4NF expresses itself to the same extent as its

wild-type counterpart. It should be noted there was no full saturation observed in these assays, therefore binding was fitted to an "estimated Bmax" curve.

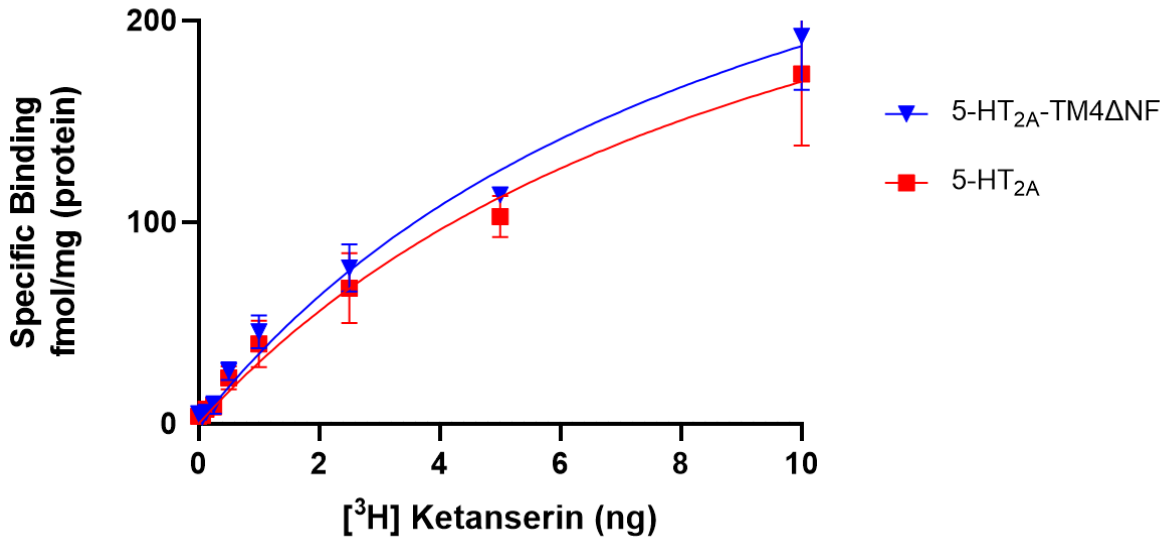

Figure 5. [3H] Ketanserin saturation binding. *Binding saturation curves in 5-HT$_{2A}$ wild type (red) and 5-HT$_{2A}$ -ΔTM4NF (blue). The binding of radioligand is plotted as a function of radioligand concentration. Specific binding was obtained by subtracting non-specific binding from total binding. All binding concentrations represent the mean – S.E.M. (n = 3; independent experiments performed in duplicate)*

Subcellular Localization of 5-HT$_{2A}$-ΔTM4NF-mcherry

Finally, subcellular localization of the 5-HT$_{2A}$ -ΔTM4NF construct was investigated. For the 5-HT$_{2A}$ receptor to be functional, the receptor must be trafficked into the plasma membrane to then interact with a ligand to propagate a signal into the cell, therefore any potential changes in trafficking due to the 5-HT$_{2C}$ mutations had to be investigated. To allow for easier identification, both the WT and mutant 5-HT$_{2A}$ constructs contained a fluorescent c-terminal mCherry tag. Hoechst stain was applied to identify the nucleus before fixation. Images acquired through confocal fluorescent microscopy (Fig. 6C, 6F) show the cellular distribution of 5-HT$_{2A}$-

ΔTM4NF-mcherry is similar to the WT 5-HT_{2A}-mcherry in HEK-293 s cells. Subcellular localization of both receptors is predominantly distributed around the cell in the plasma membrane with m-cherry fluorescence also detected within another unidentified subcellular compartment(s).

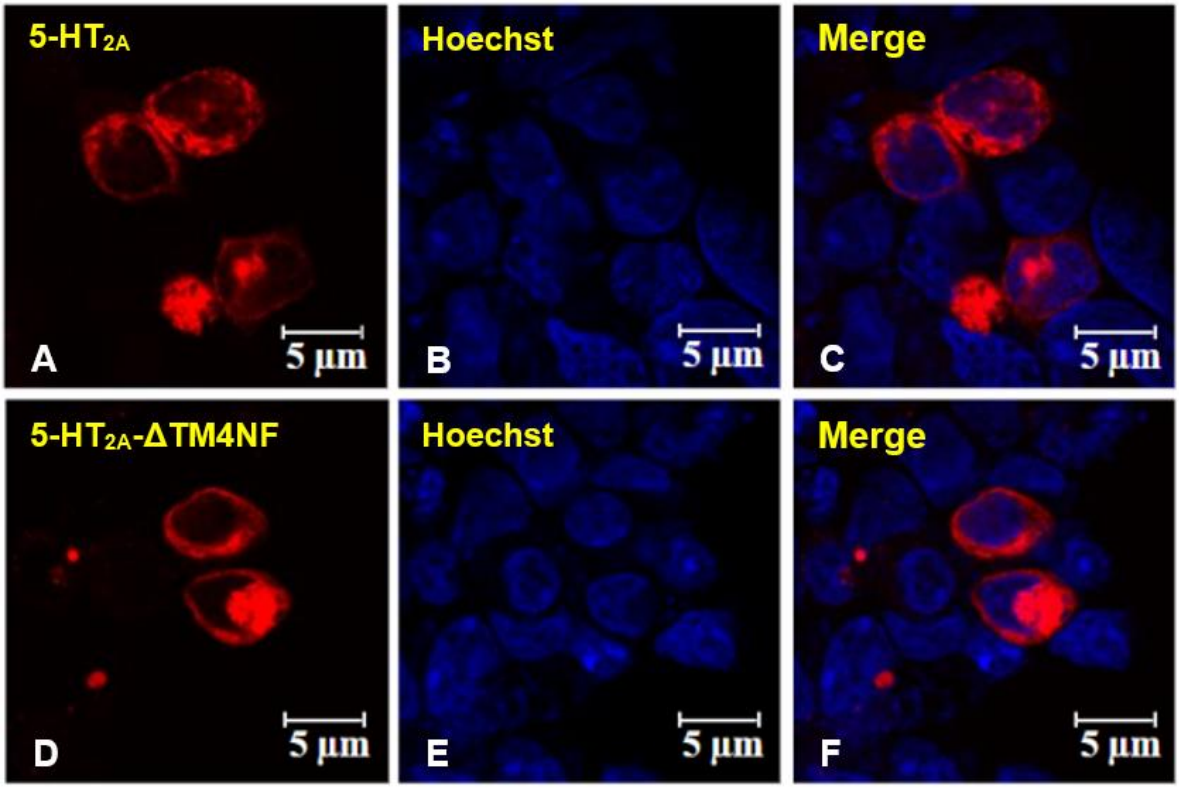

Figure 6 Cytochemistry 5-HT2A-TM4ΔNF in HEK-293 cells. *Confocal analysis highlighting the presence of 5-HT_{2A}-ΔTM4NF-mcherry receptor in transiently transfected HEK-293 cells. The figure shows representative images of six experiments.*

Chapter 4: Discussion

Although the structural interface of mGlu2 in mediating the heteromeric complex of 5-HT_{2A}·mGlu2 has been identified, the 5-HT_{2A} heteromerization residues have only been narrowed down to the TM4 domain. This study provides evidence for the involvement of four residues

located at the intracellular end of TM4 within 5-HT_{2A} in its heteromeric assembly with the mGlu2 receptor.

These findings indicate the residues F4.43, L4.44, I4.47, and A4.48 of 5-HT_{2A}, which are oriented facing the lipid bilayer, play a critical role in the expression of the heteromeric complex with mGlu2 in HEK-293 cells. Replacing these four residues with those in the TM4 of the closely similar 5-HT2C significantly disrupts its heteromeric association with the 5-HT_{2A} receptor (Fig. 3A). Functional and structural assays performed in this study verify the expression of the 5-HT_{2A}-TM4ΔNF is homologous to 5-HT_{2A}; therefore, the reduced signal observed in the co-immunoprecipitation immunoblot assay can be attributed to a disruption in the heteromeric association rather than a decrease in the level of expression. It should be noted, the sample size used in this study was relatively small (n=3). Nevertheless, these findings suggest that N-terminal residues are critical structural components mediating heteromeric formation. It is important to mention the present evidence does not exclude the possibility other residues not in the N-terminal half of TM4 still maintain the heteromeric interface. It is also possible 5-HT_{2A} and mGlu2 receptors interact indirectly as a part of a larger protein complex, by way-of scaffolding proteins, rather than interacting directly as a part of a GPCR heteromeric complex.

To verify the overall quaternary structure of the receptor had not been disrupted with the introduction of 5-HT_{2C} residues, Western blot assays were performed. This confirmed structure and expression of 5-HT_{2A}-TM4ΔNF was homologous to 5-HT_{2A}. While two anti-myc immunoreactive bands were detected, statistical analysis was performed only on the 250 kDa (pentamer) signal. This was due to the co-immunoprecipitated immunoblot assay revealing no monomeric signal, and analysis was to maintain consistency between experiments (Fig 2B).

Cross-talk plays a critical role in forming a G_i/G_q balance between the 5-HT_{2A} and mGlu2 receptors. Therefore, when characterizing the 5-HT_{2A}-TM4ΔNF mutant chimera, it was necessary to confirm the mutation did not cause dysfunctionality in signaling. Ca^{2+} mobilization confirmed that the 5-HT_{2A}-TM4ΔNF mutant forms a functional receptor that is functionally homologous to WT 5-HT_{2A}. Further cross-talk studies, as described in Moreno *et al*. (2016), could be used to verify the disruption of the heteromeric complex observed in the co-immunoprecipitation (Fig. 3). A failure or reduction in the Ca^{2+} signal induced by activation of the mGlu2 receptor would confirm the results observed in this study, suggesting the heteromeric interface has been disrupted significantly.

A potential explanation for the reduced signal detected in this study could be the 5-HT_{2A}-TM4ΔNF receptor does not properly get trafficked into the membrane, and therefore does not form an interaction with mGlu2. This possibility was investigated using confocal fluorescence microscopy, verifying the 2A/2C chimera showed proper subcellular localization following translation. mCherry fluorescence was detected predominantly in the plasma membrane, with other signals detected in unidentified cellular compartment(s). Before being trafficked into the plasma membrane, 5-HT_{2A} plasmids are first translated in the endoplasmic reticulum (ER). Therefore, the concentrated fluorescence not surrounding the cell is likely localized in the ER. To verify this, immunocytochemistry can be performed staining for an ER-resident protein (e.g., calreticulin) and the 5-HT_{2A}-TM4ΔNF receptor.

It would also be interesting to image 5-HT_{2A}-TM4ΔNF co-transfected with mGlu2 to verify the disruption of the heteromer via an absence of co-localization as described in Gonzalez-Maeso et al. (2008).

This study utilized human embryonic kidney cells (*HEK-293*) as a heterologous expression system, as it allows for highly reproducible results and maintains consistency with previous studies investigating the 5-HT_{2A}·mGlu2 complex in vitro (Moreno *et al*., 2012; Gonzalez-Maeso et al., 2008; Thibado *et al*., 2021). It is appropriate to recognize a potential limitation when using HEK-293 cells as an expression system. When cells are cultured for an extended period of time, their health deteriorates. This has an effect on the cell's growth rate and translation efficiency, which might have a negative effect on the overall study, including the repeatability of results (Thomas *et al*., 2005; Dumont *et al*., 2016). With this in mind, the maximum passage number was kept below 20 throughout this study.

The main limitation of this study is the relatively small number of assays used to verify a disruption in the heterocomplex. In terms of future research, it would be interesting to confirm the current findings with biophysical assays such as BRET and FRET (Moreno *et al*., 2016). It should be noted these methods most commonly used to assess GPCR homo- or hetero-dimerization, including co-immunoprecipitation, cannot demonstrate direct physical proximity between two receptors. Protein to protein interactions detected by these techniques could instead be facilitated by a third unknown protein that associates all the proteins into a larger complex, rather than being in direct physical proximity between the two receptors.

Much work remains to be done before a complete understanding of the 5-HT_{2A}·mGlu2 heteromeric interface is established. While this study provides valuable information on TM4 residues implicated in heteromer formation, alone, it does not provide sufficient evidence to confirm the residues mutated in the 5-HT_{2A}-TM4ΔNF form a direct interaction with mGlu2. As the co-immunoprecipitation assay revealed a significant reduction in immunoreactivity but not an absence of a band altogether, it can be assumed there may be other residues located in the C-

terminal end of TM4 that also mediate the formation of the 5-HT_{2A}·mGlu2 complex. Therefore, other constructs mutating non-homologous residues in the C-terminal half of TM4 could be created and co-immunoprecipitated with mGlu2 to determine whether other residues also play a role in mediating the heteromeric interface. It could also be possible not all four mutations found in 5-HT_{2A}-TM4ΔNF are necessary to disrupt the dimeric interface. This may be addressed by introducing single point mutations of F4.43, L4.44, A4.47, and I4.48 to create four separate constructs to determine whether one of these residues alone produces a significant disruption in the co-immunoprecipitation signal. While the 5-HT_{2A}-TM4ΔNF construct mutated four residues in the N terminal half of TM4, it is possible even a partial mutant, where only two residues were mutated (e.g., I4.47 and A4.48), could be sufficient in disrupting the binding interface of the heteromer.

As 5-HT_{2C} does not form a heterocomplex with mGlu2, it would also be interesting to introduce the 5-HT_{2A} receptor residues (F4.43, L4.44, A4.47, and I4.48) into the 5-HT_{2C} receptor to try to revive dimerization. This would provide further evidence for these residues' role in mediating the heteromeric interface.

While commonly used methods to assess GPCR homo/heteromerization are mostly indirect approaches, a photocrosslinking technique can identify individual amino acids that interact physically at the heteromeric interface without compromising the overall structural integrity of either protomer in the complex (Shah *et al*., 2020). For example, four new constructs correspond to the four residues used to create the 5-HT_{2A}-TM4NF construct, could be refined to include a single photoreactive unnatural amino acid corresponding to F4.43, L4.44, A4.47, or I4.48 corresponding to each of the four new constructs. These constructs could then undergo UV-mediated crosslinking, which would reveal whether one or more of the four residues mutated in

this study form a direct interaction with mGlu2 and participate directly in establishing the heteromeric interface of the 5-HT_{2A}-mGlu2 complex.

Although the current results must be verified by future research, the present study has provided clear evidence for the involvement of the N-terminal end of TM4 of the 5-HT_{2A} receptor in its heteromeric assembly with the mGlu2 receptor and provides a good starting point for further studies.

Conclusion:

- Sequence analysis of 5-HT_{2A}-ΔTM4NF verifies the construct contains the 5-HT_{2C} receptor residues located at the N-terminal of the TM4.
- Immunoblot experiments conducted in this study verify the similar expression of 5-HT_{2A}-ΔTM4NF and WT 5-HT_{2A}
- 5-HT_{2A}-TM4NF/mGlu2 co-immunoprecipitation was significantly reduced, suggesting the heteromeric interface had been disrupted.
- Functional homology was verified through Ca^{2+} mobilization, displaying a similar pattern of Ca^{2+} release between the 5-HT_{2A}-ΔTM4NF and WT 5-HT_{2A}
- [^{3}H]ketanserin binding confirmed receptor density and affinity similarity between 5-HT_{2A}-TM4NF and WT 5-HT_{2A}.
- Cytochemistry confirmed the 5-HT_{2A}-ΔTM4NF mutant has proper subcellular localization.
- Further analysis to confirm the findings includes BRET, FRET, and fluorescent microscopy of 5-HT_{2A}-ΔTM4NF/mGlu2 co-transfected HEK-293 cells.

- Future work in using a photocrosslinking technique to identify the individual residues responsible for the heteromeric interface

References

1. Abi-Dargham A, Rodenhiser J, Printz D, et al (2000) Increased baseline occupancy of D2 receptors by dopamine in schizophrenia. Proc Natl Acad Sci U S A 97:8104–8109. https://doi.org/10.1073/pnas.97.14.8104

2. American Psychiatric Association (2013) Diagnostic and Statistical Manual of Mental Disorders, 5th ed. American Psychiatric Association

3. Ballesteros JA, Weinstein H (1995) Methods in Neurosciences. Academy Press 25:366–428

4. Bjarnadóttir TK, Gloriam DE, Hellstrand SH, et al (2006) Comprehensive repertoire and phylogenetic analysis of the G protein-coupled receptors in human and mouse. Genomics 88:263–273. https://doi.org/10.1016/j.ygeno.2006.04.001

5. Brink CB, Harvey BH, Bodenstein J, et al (2004) Recent advances in drug action and therapeutics: Relevance of novel concepts in G-protein-coupled receptor and signal transduction pharmacology. Br J Clin Pharmacol 57:373–387. https://doi.org/10.1111/j.1365-2125.2003.02046.x

6. Brisch R, Saniotis A, Wolf R, et al (2014) The role of dopamine in schizophrenia from a neurobiological and evolutionary perspective: Old fashioned, but still in vogue. Front. Psychiatry 5

7. Cartmell J, Schoepp DD (2000) Regulation of Neurotransmitter Release by Metabotropic Glutamate Receptors. Conn and Pin

8. Charlson FJ, Ferrari AJ, Santomauro DF, et al (2018) Global epidemiology and burden of schizophrenia: Findings from the global burden of disease study 2016. Schizophr Bull 44:1195–1203. https://doi.org/10.1093/schbul/sby058

9. Conn PJ, Lindsley CW, Jones CK (2009) Activation of metabotropic glutamate receptors as a novel approach for the treatment of schizophrenia. Trends Pharmacol Sci 30:25–31. https://doi.org/10.1016/j.tips.2008.10.006

10. Crismon L, Buckley P (2014) Schizophrenia. In: DiPiro J, Talbert R, Yee G (eds) Pharmacotherapy: A Pathophysiologic Approach, 9th ed. McGraw-Hill, New York, pp 1019–1046

11. Davis KL, Kahn RS, Ko G, Davidson M (1991) Dopamine in schizophrenia: a review and reconceptualization. Am J Psychiatry 148:1474–1486. https://doi.org/10.1176/ajp.148.11.1474

12. Delille HK, Becker JM, Burkhardt S, et al (2012) Heterocomplex formation of 5-HT2A-mGlu2 and its relevance for cellular signaling cascades. Neuropharmacology 62:2184–2191. https://doi.org/10.1016/j.neuropharm.2012.01.010

13. Dimri, S., Basu, S., & De, A. (2016). Use of Bret to study protein–protein interactions in vitro and in vivo. *Methods in Molecular Biology*, 57–78. https://doi.org/10.1007/978-1-4939-3724-0_5

14. Dumont J, Euwart D, Mei B, et al (2016) Human cell lines for biopharmaceutical manufacturing: history, status, and future perspectives. Crit Rev Biotechnol 36:1110–1122. https://doi.org/10.3109/07388551.2015.1084266

15. Farde L, Nordstr A-L, Wiesel F-A, et al (1992) Positron Emission Tomographic Analysis of Central D1 and D2 Dopamine Receptor Occupancy in Patients Treated With Classical Neuroleptics and Clozapine Relation to Extrapyramidal Side Effects. Arch Gen Psychiatry 49:538–544

16. Filippov AK, Couve AS, Pangalos MN, et al (2000) Heteromeric Assembly of GABA B R1 and GABA B R2 Receptor Subunits Inhibits Ca 2 Current in Sympathetic Neurons

17. Foster DJ, Conn PJ (2017) Allosteric Modulation of GPCRs: New Insights and Potential Utility for Treatment of Schizophrenia and Other CNS Disorders. Neuron 94:431–446. https://doi.org/10.1016/j.neuron.2017.03.016

18. Freedman R, Olincy A, Ross RG, et al (2003) The genetics of sensory gating deficits in schizophrenia. Curr Psychiatry Rep 5:155–161. https://doi.org/10.1007/s11920-003-0032-2

19. Fribourg M, Moreno JL, Holloway T, et al (2011) Decoding the Signaling of a GPCR Heteromeric Complex Reveals a Unifying Mechanism of Action of Antipsychotic Drugs. Cell 147:1011–1023. https://doi.org/10.1016/j.cell.2011.09.055

20. Friedman JI, Temporini H, Davis KL (1999) Pharmacologic strategies for augmenting cognitive performance in schizophrenia. Biol Psychiatry 45:. https://doi.org/10.1016/S0006-3223(98)00287-X

21. Geyer MA, Vollenweider FX (2008) Serotonin research: Contributions to understanding psychoses. Trends Pharmacol. Sci. 29:445–453

22. Gogtay N, Vyas NS, Testa R, et al (2011) Age of onset of schizophrenia: Perspectives from structural neuroimaging studies. Schizophr Bull 37:504–513. https://doi.org/10.1093/schbul/sbr030

23. González-Maeso J, Ang RL, Yuen T, et al (2008) Identification of a serotonin/glutamate receptor complex implicated in psychosis. Nature 452:93–97. https://doi.org/10.1038/nature06612

24. González-Maeso J, Weisstaub N V., Zhou M, et al (2007) Hallucinogens Recruit Specific Cortical 5-HT2A Receptor-Mediated Signaling Pathways to Affect Behavior. Cell Press 53:439–452. https://doi.org/10.1016/j.neuron.2007.01.008

25. González-Maeso J, Yuen T, Ebersole BJ, et al (2003) Cellular/Molecular Transcriptome Fingerprints Distinguish Hallucinogenic and Nonhallucinogenic 5-Hydroxytryptamine 2A Receptor Agonist Effects in Mouse Somatosensory Cortex. J Neurosci 23:8836–8843

26. Greenberg PE, Fournier AA, Sisitsky T, et al (2015) The economic burden of adults with major depressive disorder in the United States (2005 and 2010). J Clin Psychiatry 76:155–162. https://doi.org/10.4088/JCP.14m09298

27. Grundmann M, Merten N, Malfacini D, et al (2018) Lack of beta-arrestin signaling in the absence of active G proteins. Nat Commun 9:. https://doi.org/10.1038/s41467-017-02661-3

28. Halberstadt AL, Koedood L, Powell SB, Geyer MA (2011) Differential contributions of serotonin receptors to the behavioral effects of indoleamine hallucinogens in mice. J Psychopharmacol 25:1548–1561. https://doi.org/10.1177/0269881110388326

29. Han Y, Moreira IS, Urizar E, et al (2009) Allosteric communication between protomers of dopamine class A GPCR dimers modulates activation. Nat Chem Biol 5:688–695. https://doi.org/10.1038/nchembio.199

30. Hor K, Taylor M (2010) Review: Suicide and schizophrenia: a systematic review of rates and risk factors. J Psychopharmacol 24:81–90. https://doi.org/10.1177/1359786810385490

31. Howes OD, Kapur S (2009) The dopamine hypothesis of schizophrenia: Version III - The final common pathway. Schizophr. Bull. 35:549–562

32. Ji TH, Grossmann M, Ji I (1998) G Protein-coupled Receptors. J Biol Chem 273:17299–17302. https://doi.org/10.1074/jbc.273.28.17299

33. Jones KA, Tamm JA, Craig DA, et al (2000) Signal Transduction by GABA B Receptor Heterodimers

34. Jordan BA, Devi LA (1999) G-protein-coupled receptor heterodimerization modulates receptor function. Nature 399:697–700. https://doi.org/10.1038/21441

35. Kapur S, Seeman P (2002) NMDA receptor antagonists ketamine and PCP have direct effects on the dopamine D2 and serotonin 5-HT2 receptors - Implications for models of schizophrenia. Mol Psychiatry 7:837–844. https://doi.org/10.1038/sj.mp.4001093

36. Kapur S, Zipursky RB, Remington G (1999) Clinical and Theoretical Implications of 5-HT 2 and D 2 Receptor Occupancy of Clozapine, Risperidone, and Olanzapine in Schizophrenia

37. Kareem MAA (2020) Exploring the Heteromeric Interface of the 5-HT2A-mGlu2 Receptor Complex. Virginia Commonwealth University

38. Kim JS, Kornhuber HH, Schmid-Burgk W, Holzmoller B (1980) Low cerebrospinal fluid glutamate in schizophrenic patients and a new hypothesis on schizophrenia

39. Kimura KT, Asada H, Inoue A, Kadji FMN, Im D, Mori C, Arakawa T, Hirata K, Nomura Y, Nomura N, Aoki J, Iwata S, Shimamura T. Structures of the 5-HT_{2A} receptor in complex with the antipsychotics risperidone and zotepine. Nat Struct Mol Biol. 2019 Feb;26(2):121-128. doi: 10.1038/s41594-018-0180-z. Epub 2019 Feb 4. PMID: 30723326.

40. Kniazeff J, Prézeau L, Rondard P, et al (2011) Dimers and beyond: The functional puzzles of class C GPCRs. Pharmacol Ther 130:. https://doi.org/10.1016/j.pharmthera.2011.01.006

41. Kryszkowski W, Boczek T (2021) The G Protein-Coupled Glutamate Receptors as Novel Molecular Targets in Schizophrenia Treatment—A Narrative Review. J Clin Med 10:1475. https://doi.org/10.3390/jcm10071475

42. Kurita M, García-Bea A, González-Maeso J (2016) Novel Targets for Drug Treatment in Psychiatry. In: The Medical Basis of Psychiatry. Springer New York, New York, NY

43. Kurita M, Holloway T, García-Bea A, et al (2012) HDAC2 regulates atypical antipsychotic responses through the modulation of mGlu2 promoter activity. Nat Neurosci 15:1245–1254. https://doi.org/10.1038/nn.3181

44. Kuszak AJ, Pitchiaya S, Anand JP, et al (2009) Purification and Functional Reconstitution of Monomeric μ-Opioid Receptors. J Biol Chem 284:26732–26741. https://doi.org/10.1074/jbc.M109.026922

45. Kwan C, Frouni I, Nuara SG, et al (2021) Combined 5-HT2A and mGlu2 modulation for the treatment of dyskinesia and psychosis in Parkinson's disease. Neuropharmacology 186:. https://doi.org/10.1016/j.neuropharm.2021.108465

46. Lacro JP, Dunn LB, Dolder CR, et al (2002) Prevalence of and Risk Factors for Medication Nonadherence in Patients With Schizophrenia. J Clin Psychiatry 63:. https://doi.org/10.4088/JCP.v63n1007

47. Levoye A, Dam J, Ayoub MA, et al (2006) Do orphan G-protein-coupled receptors have ligand-independent functions? EMBO Rep 7:1094–1098. https://doi.org/10.1038/sj.embor.7400838

48. Liang Y-L, Khoshouei M, Radjainia M, et al (2017) Phase-plate cryo-EM structure of a class B GPCR–G-protein complex. Nature 546:118–123. https://doi.org/10.1038/nature22327

49. Liu N, Wang Y, Li T, Feng X (2021) G-protein coupled receptors (Gpcrs): Signaling pathways, characterization, and functions in insect physiology and toxicology. Int J Mol Sci 22:. https://doi.org/10.3390/ijms22105260

50. Llansola M, Sánchez-Pérez AM, Montoliu C, Felipo V (2004) Modulation of NMDA receptor function by cyclic AMP in cerebellar neurones in culture. J Neurochem 91:591–599. https://doi.org/10.1111/j.1471-4159.2004.02730.x

51. Łukasiewicz S, Polit A, Kędracka-Krok S, et al (2010) Hetero-dimerization of serotonin 5-HT2A and dopamine D2 receptors. Biochim Biophys Acta - Mol Cell Res 1803:. https://doi.org/10.1016/j.bbamcr.2010.08.010

52. Meltzer HY, Bastani B, Kwon KY, et al (1989) A prospective study of clozapine in treatment-resistant schizophrenic patients I. Preliminary report

53. Meltzer H, Kostacoglu A (2001) Treatment-resistant schizophrenia. In: Lieberman J, Murray R (eds) Comprehensive Care of Schizophrenia: A Textbook of Clinical Management. Martin Dunitz, London, pp 181–203

54. Miller A, McEvoy J, Jester D (2006) Treatment of chronic schizophrenia. In: Lieberman J, Stroup T, Perkins D (eds) Textbook of Schizophrenia. American Psychiatric Publishing, Washington, DC, pp 365–381

55. Mishra A, Singh S, Shukla S (2018) Physiological and Functional Basis of Dopamine Receptors and Their Role in Neurogenesis: Possible Implication for Parkinson's disease. J. Exp. Neurosci. 12

56. Miyamoto S, Duncan GE, Marx CE, Lieberman JA (2005) Treatments for schizophrenia: a critical review of pharmacology and mechanisms of action of antipsychotic drugs. Mol Psychiatry 10:79–104. https://doi.org/10.1038/sj.mp.4001556

57. Moghaddam B (2004) Targeting metabotropic glutamate receptors for treatment of the cognitive symptoms of schizophrenia. Psychopharmacology (Berl). 174:39–44

58. Moreno JL, Holloway T, Albizu L, et al (2011) Metabotropic glutamate mGlu2 receptor is necessary for the pharmacological and behavioral effects induced by hallucinogenic 5-HT2A receptor agonists. Neurosci Lett 493:76–79. https://doi.org/10.1016/j.neulet.2011.01.046

59. Moreno JL, Miranda-Azpiazu P, García-Bea A, et al (2016) Allosteric signaling through an mGlu2 and 5-HT $_{2A}$ heteromeric receptor complex and its potential contribution to schizophrenia. Sci Signal 9:. https://doi.org/10.1126/scisignal.aab0467

60. Moreno JL, Muguruza C, Umali A, et al (2012) Identification of Three Residues Essential for 5-Hydroxytryptamine 2A-Metabotropic Glutamate 2 (5-HT2A·mGlu2) Receptor Heteromerization and Its Psychoactive Behavioral Function. J Biol Chem 287:44301–44319. https://doi.org/10.1074/jbc.M112.413161

61. Nordstrom A-L, Farde L, Nyberg S, et al (1995) D1, D2, and 5-HT2 Receptor Occupancy in Relation to Clozapine Serum Concentration: A PET Study of Schizophrenic Patients

62. Olfson M, Gerhard T, Huang C, et al (2015) Premature Mortality Among Adults With Schizophrenia in the United States. JAMA Psychiatry 72:1172. https://doi.org/10.1001/jamapsychiatry.2015.1737

63. Owen MJ, Sawa A, Mortensen PB (2016) Schizophrenia. Lancet 388:86–97. https://doi.org/10.1016/S0140-6736(15)01121-6

64. Patel KR, Cherian J, Gohil K, Atkinson D (2014) Schizophrenia: overview and treatment options. P T 39:638–45

65. Patil ST, Zhang L, Martenyi F, et al (2007) Activation of mGlu2/3 receptors as a new approach to treat schizophrenia: A randomized Phase 2 clinical trial. Nat Med 13:1102–1107. https://doi.org/10.1038/nm1632

66. Ripke S, O'Dushlaine C, Chambert K, et al (2013) Genome-wide association analysis identifies 13 new risk loci for schizophrenia. Nat Genet 45:1150–1159. https://doi.org/10.1038/ng.2742

67. Rives M-L, Vol C, Fukazawa Y, et al (2009) Cross-talk between GABAB and mGlu1a receptors reveals new insight into GPCR signal integration. EMBO J 28:2195–2208. https://doi.org/10.1038/emboj.2009.177

68. Rosenbaum DM, Rasmussen SGF, Kobilka BK (2009) The structure and function of G-protein-coupled receptors. Nature 459:356–363. https://doi.org/10.1038/nature08144

69. Rotaru DC, Yoshino H, Lewis DA, et al (2011) Glutamate receptor subtypes mediating synaptic activation of prefrontal cortex neurons: Relevance for schizophrenia. J Neurosci 31:142–156. https://doi.org/10.1523/JNEUROSCI.1970-10.2011

70. Saha S, Chant D, McGrath J (2007) A Systematic Review of Mortality in Schizophrenia. Arch Gen Psychiatry 64:1123. https://doi.org/10.1001/archpsyc.64.10.1123

71. Salomon JA, Haagsma JA, Davis A, et al (2015) Disability weights for the Global Burden of Disease 2013 study. Lancet Glob Heal 3:e712–e723. https://doi.org/10.1016/S2214-109X(15)00069-8

72. Schreiber R, Brocco M, Millan MJ (1994) Blockade of the discriminative stimulus effects of DOI by MDL 100,907 and the "atypical" antipsychotics, clozapine and risperidone

73. Shah UH, Toneatti R, Gaitonde SA, et al (2020) Site-Specific Incorporation of Genetically Encoded Photo-Crosslinkers Locates the Heteromeric Interface of a GPCR Complex in Living Cells. Cell Chem Biol 27:1308-1317.e4. https://doi.org/10.1016/j.chembiol.2020.07.006

74. Stępnicki P, Kondej M, Kaczor AA (2018) Current concepts and treatments of schizophrenia. Molecules 23:. https://doi.org/10.3390/molecules23082087

75. Swanson CJ, Bures M, Johnson MP, et al (2005) Metabotropic glutamate receptors as novel targets for anxiety and stress disorders. Nat. Rev. Drug Discov. 4:131–144

76. Tallerico T, Novak G, Liu ISC, et al (2001) Schizophrenia: elevated mRNA for dopamine D2Longer receptors in frontal cortex. Mol Brain Res 87:. https://doi.org/10.1016/S0169-328X(00)00293-X

77. Tang, Z., & Takahashi, Y. (2018). Analysis of protein–protein interaction by Co-IP in human cells. *Methods in Molecular Biology*, 289–296. https://doi.org/10.1007/978-1-4939-7871-7_20

78. Thibado JK, Tano J-Y, Lee J, et al (2021) Differences in interactions between transmembrane domains tune the activation of metabotropic glutamate receptors. Elife 10:. https://doi.org/10.7554/eLife.67027

79. Thomas P, Smart TG (2005) HEK293 cell line: A vehicle for the expression of recombinant proteins. J Pharmacol Toxicol Methods 51:187–200. https://doi.org/10.1016/j.vascn.2004.08.014

80. Toda M, Abi-Dargham A (2007) Dopamine hypothesis of schizophrenia: Making sense of it all. Curr Psychiatry Rep 9:. https://doi.org/10.1007/s11920-007-0041-7

81. Traynelis SF, Wollmuth LP, McBain CJ, et al (2010) Glutamate receptor ion channels: Structure, regulation, and function. Pharmacol. Rev. 62:405–496

82. Urban JD, Clarke WP, Von Zastrow M, et al (2007) Functional selectivity and classical concepts of quantitative pharmacology. J. Pharmacol. Exp. Ther. 320:1–13

83. Vassilatis DK, Hohmann JG, Zeng H, et al (2003) The G protein-coupled receptor repertoires of human and mouse. Proc Natl Acad Sci 100:4903–4908. https://doi.org/10.1073/pnas.0230374100

84. Wander C (2020) Schizophrenia: opportunities to improve outcomes and reduce economic burden through managed care. Am J Manag Care 26:. https://doi.org/10.37765/ajmc.2020.43013

85. Whorton MR, Bokoch MP, Rasmussen SGF, et al (2007) A monomeric G protein-coupled receptor isolated in a high-density lipoprotein particle efficiently activates its G protein. Proc Natl Acad Sci 104:7682–7687. https://doi.org/10.1073/pnas.0611448104

86. Wise A, Gearing K, Rees S (2002) Target validation of G-protein coupled receptors. Drug Discov Today 7:235–246. https://doi.org/10.1016/S1359-6446(01)02131-6

87. Wootten D, Christopoulos A, Marti-Solano M, et al (2018) Mechanisms of signalling and biased agonism in G protein-coupled receptors. Nat Rev Mol Cell Biol 19:638–653. https://doi.org/10.1038/s41580-018-0049-3

88. Zeng F, Wess J (2000) Molecular Aspects of Muscarinic Receptor Dimerization. Neuropsychopharmacology 23:S19–S31. https://doi.org/10.1016/S0893-133X(00)00146-9